

Vibrational excitations of As_2O_3 . II. Crystalline phases

E. J. Flynn and S. A. Solin*

The James Franck Institute and The Department of Physics, The University of Chicago, Chicago, Illinois 60637

G. N. Papatheodorou

Chemical Engineering Division, Argonne National Laboratory, Argonne, Illinois 60439

(Received 7 July 1975)

Infrared absorption and polarized Raman spectra of monoclinic As_2O_3 and the room temperature Raman spectrum of cubic As_2O_3 have been recorded. A number of vibrational features possessed by the crystalline modifications of arsenic trioxide are common to crystals of As_2S_3 and As_2Se_3 , but have been resolved in greater detail. In particular, the layered monoclinic phase, claudetite, exhibited rigid layer modes at Raman shifts of 30, 38, and 49 cm^{-1} , and numerous Davydov doublets, all of which appeared as a consequence of weak layer-layer coupling. Oriented samples of claudetite yielded polarized Raman measurements which did not obey the symmetry-determined selection rules of the $C_{2h}^5-P2_1/n$ space group for reasons which can be traced to the fact that claudetite is biaxial. However, the vibrational frequencies of claudetite scale consistently to those of monoclinic As_2S_3 and As_2Se_3 by scaling factors of 0.82 and 0.58, respectively. Thus, many claudetite lines are related by the empirical scaling result to As_2S_3 modes belonging to vibrational species which have been identified by infrared reflectivity measurements. Recurring bands in the ordered and disordered phases of As_2O_3 are noted and structural similarities between the different phases are evidenced by vibrational features that are comparable in frequency and symmetry. Accordingly, layered structure in arsenic trioxide glass is inferred.

I. INTRODUCTION

The various amorphous and crystalline forms of As_2O_3 are closely similar to those of the other arsenic chalcogenides. Corresponding to the semiconducting glasses and liquids of As_2S_3 and As_2Se_3 are the disordered versions of As_2O_3 , the vibrational spectra of which were treated in the preceding paper. The bulk of the present discussion is devoted to monoclinic As_2O_3 ("claudetite"), a biaxial layered material which exhibits several important features common to like crystals of As_2S_3 and As_2Se_3 . Most striking is the persistence of simple frequency scaling between vibrations of arsenic trioxide, trisulfide, and triselenide, despite ostensibly essential differences in strong intralayer bonding characteristics. Moreover, the weakness of layer-layer coupling, inherent to correlation field or Davydov splitting and low-frequency rigid-layer modes, renders the molecular symmetry of the layer experimentally discernable.

Cubic As_2O_3 ("arsenolite") has been thoroughly studied by others. Nevertheless, for completeness and for the purpose of comparison with claudetite, we will also present and briefly discuss our Raman studies of arsenolite.

II. EXPERIMENTAL

Crystals of claudetite were vapor grown by first sealing a drop of water and a small amount of commercially prepared arsenolite powder in an evacuated quartz tube ($\sim \frac{1}{4}$ in. diam \times 5 in. long). To avoid boiling off the water when the vacuum was

pulled, one end of the tube, in which the ingredients were isolated, was immersed in liquid nitrogen while the other end was closed just below the vacuum hose. The sealed tube was heated non-uniformly at about 200 $^\circ\text{C}$ for several weeks. The powder, at one end, was maintained at a relatively elevated temperature. As_2O_3 which sublimed across a 10 $^\circ$ -20 $^\circ$ temperature gradient to the cool end crystallized as monoclinic claudetite. The remaining arsenolite powder transformed to a sintered chunk of claudetite whiskers from which a powder was prepared for infrared work.

Infrared absorption spectra of claudetite were recorded on a Digilab Fourier-transform spectrometer (FTS). Each FTS absorption curve, in fact, represents the point-by-point ratio of two transmission spectra: that of a claudetite-nujol mull on a polyethylene substrate and a reference spectrum of nujol on polyethylene. The absorption spectrum of claudetite from 20 to 1000 cm^{-1} was obtained in three separate scans covering the near, mid, and far ir.

Transmission Raman spectra were excited by the 5145- \AA argon ion laser line with ~ 58 -mW incident radiation. The scattered light was analyzed at 90 $^\circ$ with a Jarrell-Ash 25-100 double monochromator (Jobin-Yvon 1800-groove/mm holographic gratings blazed at 0.5 μ), RCA C31034 phototube, and photon counting electronics.

The Raman spectra of claudetite were obtained from a very delicate (thickness < 10 μ), transparent platelet that was oriented on a Buerger precession x-ray camera.¹ The relationship between the crystallographic axes a , b , and c in the

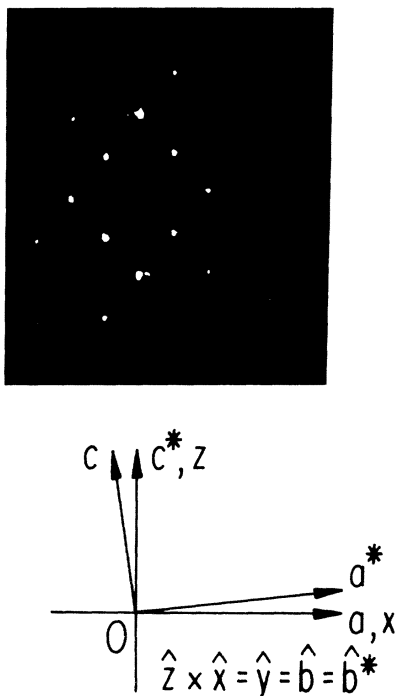


FIG. 1. Orientation photograph of claudetite. Below the x-ray photograph, the crystallographic axes are referred to a set of Cartesian coordinates (xyz) . Asterisks label directions in reciprocal space. Angle $c0a = 94^\circ$.

oriented sample and a set of Cartesian coordinates to which we refer scattering and polarization configurations is illustrated in Fig. 1. In accordance with the crystal principal axes defined by Nye² the optic axis b is chosen parallel to y , and the conventional³ $i(jk)l$ designations label all polarized Raman spectra reported in this paper. The Raman spectrum of mineral claudetite⁴ (from Schmölnitz, Hungary) was also recorded and found to be identical to that of the synthetic sample. No polarization measurements of the observed Raman lines of the natural sample were made.

Preparation of arsenolite crystals was described in the preceding paper. The Raman spectrum of arsenolite was recorded in the transmission mode, but the polarization dependence of the observed Raman-active lines was not investigated.

III. RESULTS AND DISCUSSION

The zero-level precession photograph of Fig. 1 is an undistorted magnification of the (010) reciprocal-lattice plane of claudetite. Stacked normal to the b axis (into the page) are the layers, two per tetramolecular unit cell, each possessing three-dimensional diperiodic symmetry.^{5,6} The in-plane spacings of the regular lattice, $a = 5.25 \text{ \AA}$ and $c = 4.54 \text{ \AA}$, and the angle $\beta = 94^\circ$ can be measured directly from the photograph. Each diffrac-

tion spot is assigned indices $(h 0 l)$ satisfying $h + l = 2n$ for nonextinction, symptomatic of $\frac{1}{2}a + \frac{1}{2}c$ or n -glide reflection symmetry (σ_1). The glide-plane operation maps the layer into itself and, together with the identity (E), characterizes the layer symmetry and its isomorphic point group C_s . The elements of the crystal point group C_{2h} (space group $C_{2h}^5 - P2_1/n$) include an inversion point (i) between layers and a twofold axis of improper rotation (C_{2i}), in addition to the symmetry elements of the layer subgroup C_s .

Now the crystal and layer point groups can be correlated.⁷ In the limit of zero interlayer interaction, the normal frequencies of the crystal are those of a single layer. Individual layer modes are nondegenerate, but the double-layer unit cell introduces a second eigenvector at each single-layer eigenfrequency. Therefore, when the layer-layer forces are "turned on," the modes of this redundant structure split according to Fig. 2: 13 pairs $A' \rightarrow 13A_g + 13B_u$, 14 pairs $A'' \rightarrow 14B_g + 14A_u$. Likewise, the zero-frequency external modes $A'' + 2A'$ become three rigid translations $2B_u + A_u$ and three Raman-active, "quasiacoustic," or rigid-layer modes—two shear modes of A_g symmetry and a compressional mode of B_g symmetry.

If we picture adjacent layers moving as rigid units out of phase, either parallel to each other or along their mutual normal, the restoring force is determined by the interaction between layers. Consequently, the rigid-layer vibrations, characterized by large mode masses and weak interlayer force constants, are located at the low-frequency end of the spectrum and can be distinguished from the in-plane molecular bands. The rigid-

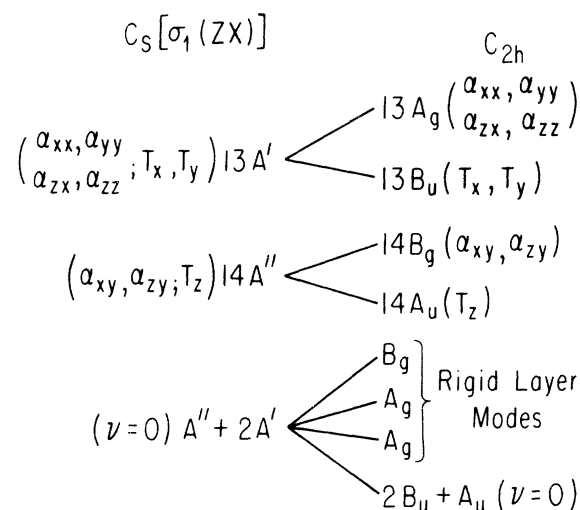


FIG. 2. Correlations and selection rules for the layer and crystal point groups.

layer motions described above transform according to their assigned symmetries and constitute exact eigenvectors of the system to the extent that anharmonic mixing with other vibrations of the same symmetry can be ignored. This approximation is enhanced by the weakness of the primarily van der Waals interlayer forces⁸ and is consistent with the isolation of the rigid-layer modes at the bottom of the spectrum.

That layer-layer coupling is weak is evidenced by the easy (010) cleavage of claudetite. A more subtle manifestation of the weak layer-layer coupling is the near coincidence of each $A_g - B_u$ and $B_g - A_u$ pair of frequencies. One member of each narrowly spaced "Davydov doublet" is Raman active (A_g or B_g) and the other infrared active. Comparison of Raman and ir spectra will show that close to each Raman frequency, excluding the rigid-layer modes, can be found a band in the infrared.

In Fig. 3 the Raman-scattering results for claudetite are reproduced. Although the spectra of Fig. 3 are dramatically polarization dependent, with pronounced extinctions and intensity reversals reflecting changes in polarization configuration, few lines obey the selection rules of Fig. 2, according to which the tensor components α_{zz} and α_{xx} are nonzero for A_g modes and zero otherwise. In contrast, α_{zy} and α_{xy} should be nonzero for B_g modes and zero otherwise. We note violations of the predictions of the selection rules at 72 cm^{-1} where $\alpha_{xy} \approx \alpha_{xz} \gg \alpha_{zz}, \alpha_{zy}$ and at the adjacent 87 cm^{-1} line where just the opposite behavior is exhibited, that is, $\alpha_{zz} \approx \alpha_{zy} \gg \alpha_{xy}, \alpha_{xz}$. Thus, unambiguous symmetry identification could not be based solely on the Raman data in all cases. The confusion stems from one or more of the following sources of difficulty: (i) Claudetite is biaxial⁹ (indices 1.87, 1.92, 2.01). Consequently the polarization of a Raman-scattered photon depends on the direction of propagation. Our collection lens subtended a large solid angle at the sample. Thus, the polarization of light scattered from a particular phonon was modified in traversing the sample, and spatially varying contributions to the polarization were superposed at the collection lens.¹⁰ (ii) Incident and scattered light suffer depolarization due to multiple reflections within the sample. Irregular sample-air interfaces are responsible for this effect. (iii) Examination of the sample under a microscope revealed cracks, local buckling of the layers, and other inhomogeneities which affected the optical quality of the crystal. In addition, a sample of claudetite could not be found that did not contain a stacking fault, as evidenced by the parasitic reflections accompanying the strong diffraction spots along the c^* axis in the x-ray photograph of Fig. 1.

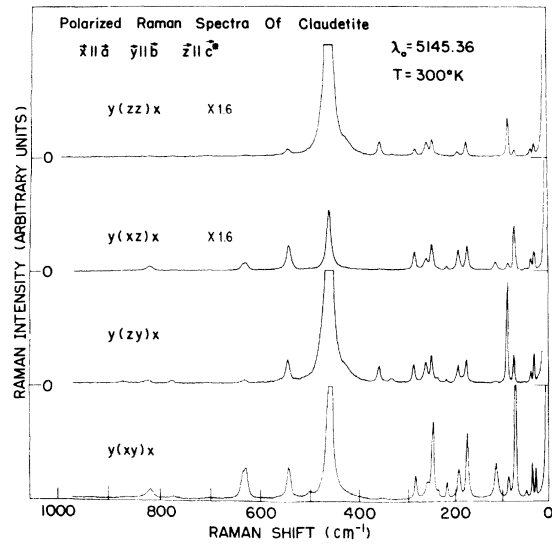


FIG. 3. Polarized Raman spectra of claudetite. $y(xy)x$ and $y(zy)x$ were recorded with a spectral slit width of 3.4 cm^{-1} . $y(zz)x$ and $y(xz)x$ were recorded with a spectral slit width of 5.7 cm^{-1} . The effective gain at which the $y(zz)x$ and $y(xz)x$ spectra were recorded was down by a factor of about 1.6 relative to that of $y(zy)x$ and $y(xy)x$ due to the dephased efficiency of the gratings for light polarized parallel to the grooves. The abscissa is linear in wavelength rather than wave number.

Addressing difficulty (i) we simply narrowed the collection aperture. The Raman signal was, of course, attenuated but the relative intensities of each of the four accessible polarization configurations were qualitatively unchanged. To alleviate difficulty (ii) the sample was immersed in a pale-yellow index matching fluid ($n = 1.87$) purchased from Cargille Laboratories, Cedar Grove, N. J. This step may have been inadequate simply because an isotropic liquid cannot ideally index match an anisotropic crystal characterized by three separate refractive indices. Thus, the crystal-fluid interfaces encountered by the Raman-scattered light were imperfectly index matched. In any case, the fluid was not fully transparent and the luminescence it produced totally obscured the Raman signal. Finally, an attempt to differentiate between polarized A_g and depolarized B_g modes in the depolarization spectrum of a pressed pellet of claudetite yielded no satisfactory results.

Polarized Raman-scattering experiments, similar to the above described measurements of claudetite in which the laser light was incident normal to the layer planes, have been performed for monoclinic As_2S_3 ("orpiment"). The geometry of the As_2O_3 and As_2S_3 polarization studies rendered accessible four independent tensor components and all four must be compared in order to conclude whether or not the polarization proper-

ties of a Raman line are compatible with the selection rules for any of the vibrational species. According to this criterion, the Raman data reported for As_2S_3 were somewhat incomplete. (None of the four components were displayed over the entire 0–400- cm^{-1} frequency range encompassing the first-order Raman spectrum of orpiment, and over no frequency range could more than two components be compared.) If, in fact, the selection rules were violated by large samples of orpiment, of much better optical quality than the claudetite crystals, the experimental difficulties posed by claudetite should not have been surprising.

A Davydov partner for nearly every Raman frequency can be found in the infrared spectra displayed in Fig. 4. Davydov doublets are listed in Table I. Absorption bands are conspicuously absent from the far ir data below 62 cm^{-1} . Most clearly resolved in the $y(xy)x$ configuration of Fig. 3 are Raman lines at 30, 38, and 49 cm^{-1} for which no Davydov components are found in the infrared. This fact decisively locates the rigid-layer modes at these three lowest Raman-active frequencies.

Frequency scaling between normal vibrations of As_2O_3 and those of As_2S_3 and As_2Se_3 is a consequence of structural similarities more basic than space-group isomorphism. Claudetite and the other arsenic chalcogenides are isostructural to the extent that a solution to the secular determinant for each compound As_2X_3 must yield identical expressions for the eigenfrequencies $\omega_k(m_{\text{As}}, m_X, \{f(\text{As}_2\text{X}_3)\})$, $k=1, 2, \dots, 60$. At the very least, it is clear that each eigenfrequency will exhibit an extremely complicated dependence on the masses, m_{As} and m_X , and force constants $\{f(\text{As}_2\text{X}_3)\}$ which differ for each crystal. Three of these frequencies are zero roots (rigid translations) and three belong to the rigid-layer vibrations. The remaining

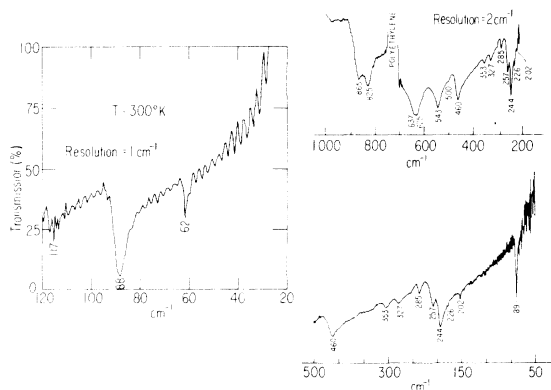


FIG. 4. Infrared absorption spectra of claudetite. Sinusoidal interference fringes are noted in the far infrared.

TABLE I. Davydov splitting in claudetite. The Raman and infrared frequencies were recorded in wave numbers to within 2 cm^{-1} .

Raman	ir	Raman	ir
30	...	285	285
38	...	331	327
49	...	357	353
72	62	426	...
87	89	461	460
114	117	501	500
174	...	544	543
192	202	633	637
217	226	773	...
236	...	818	825
248	244	869	865
260	257		

54 frequencies correspond to the 27 Raman-active intralayer modes and their infrared Davydov partners. However, severe demands on the algebraic form of the eigenfrequencies of the full As_2X_3 unit cell are imposed by the fact that the intralayer frequencies of any two As_2X_3 crystals scale by very nearly a single scaling factor. The experimental scaling result suggests that the set of intralayer eigenfrequencies can formally be written

$$\omega_k(m_{\text{As}}, m_X, \{f(\text{As}_2\text{X}_3)\}) = F(m_{\text{As}}, m_X, \{g(\text{As}_2\text{X}_3)\}) \times \omega'_k(m_{\text{As}}, m_X, \{f(\text{As}_2\text{X}_3)\}), \quad (1)$$

where $\{g(\text{As}_2\text{X}_3)\}$ is some subset of the force constants $\{f(\text{As}_2\text{X}_3)\}$. The function F has the same numerical value for all intralayer modes of a particular crystal, but the set of frequencies ω'_k , $k=1, 2, \dots, 54$ are common to all three compounds As_2O_3 , As_2S_3 , and As_2Se_3 , i. e., independent of the element X . One cannot deduce on the basis of symmetry considerations that the expressions for the eigenfrequencies can be factored in a manner compatible with intercrystal frequency scaling, but empirical information forces one to conclude that the above form obtains.

Zallen has suggested that frequency scaling between vibrations of monoclinic As_2S_3 and As_2Se_3 evolves from scaling between the bond-stretching frequencies of the AsX_3 pyramidal subunits from which the two-dimensional network layers of the monoclinic crystal are constructed. Equations from which the symmetric stretching frequency ν_1 of an AsX_3 molecule can be calculated have been given by Herzberg.¹¹ Upon solving those equations and retaining only terms to first order in k_2/k_1 , one finds

$$4\pi\nu_1^2 = \frac{k_1}{\mu_1} \left[1 + 9 \frac{k_2}{k_1} \left(\frac{\mu_1}{m_{\text{As}}} \right)^2 \cos^2\beta \sin^2\beta \right. \\ \left. \times \left(1 - \frac{k_2\mu_1}{k_1\mu_2} \right)^{-1} + \dots \right], \quad (2)$$

where

$$\frac{1}{\mu_1} = \frac{1}{m_X} + \frac{3 \cos^2 \beta}{m_{As}}, \quad (3)$$

$$\frac{1}{\mu_2} = \frac{1}{m_X} + \frac{3 \sin^2 \beta}{m_{As}},$$

and

$$k_2 = \frac{12 \cos^2 \beta}{1 + 3 \cos^2 \beta} \frac{k_b}{l^2}. \quad (4)$$

In Herzberg's notation, k_b/l^2 and k_1 are the X -As- X bond bending and As- X stretching force constants, respectively. The angle β between the As- X bond and the axis of molecular symmetry is related to the X -As- X pyramidal angle α by

$$\sin \beta = (2/\sqrt{3}) \sin \frac{1}{2} \alpha. \quad (5)$$

The ratio $(k_b/l^2)/k_1$ is typically ~ 0.1 . Therefore the relative magnitude of the second term in Eq. (1) is about 0.006 for As_2O_3 , 0.02 for As_2S_3 , and 0.07 for As_2Se_3 if $\alpha = 100^\circ$. Substituting the average valence angles $\alpha(O-As-O) = 100^\circ$, $\alpha(S-As-S) = 99^\circ$, and $^{12,13} \alpha(Se-As-Se) = 98^\circ$ into Eq. (2), we find

$$\frac{\nu_1(As_2S_3)}{\nu_1(As_2O_3)} = 0.75 \left(\frac{k_1(As_2S_3)}{k_1(As_2O_3)} \right)^{1/2}$$

and

$$\frac{\nu_1(As_2Se_3)}{\nu_1(As_2S_3)} = 0.75 \left(\frac{k_1(As_2Se_3)}{k_1(As_2S_3)} \right)^{1/2}.$$

These calculations correspond to observed scaling factors 0.82 and 0.71, respectively, and match experiment if $k_1(As_2Se_3)/k_1(As_2S_3) = 0.90$ and $k_1(As_2S_3)/k_1(As_2O_3) = 1.2$. The arsenic chalcogen bonding distances As-O = 1.80 Å, As-S = 2.24 Å, and As-Se = 2.40 Å agree qualitatively with the conclusion that the As_2Se_3 intralayer bonds are 10% weaker than these in orpiment, but contradict the result $k_1(As_2S_3)/k_1(As_2O_3) > 1$, if we assume that greater bond lengths correspond to weaker binding forces. Thus, a model that neglects coupling between the pyramidal units which compose the two-dimensional network layers of arsenic oxide, sulfide, and selenide is quantitatively inaccurate, but nevertheless roughly outlines the manner in which ubiquitous frequency scaling is rooted in structural similarities.

The above described intercrystal frequency scaling is so reliable that the vibrational species to which many As_2O_3 Raman lines belong can be deduced if we assume that scaling between As_2O_3 and As_2S_3 relates modes of like symmetry. The first column of Table II is a list of frequencies from the claudetite Raman data, each of which scales to the mean frequency of a particular As_2S_3

TABLE II. Intercrystal frequency scaling. The frequencies listed below were measured in cm^{-1} .

$\nu(As_2O_3)$	$\nu(As_2S_3)$		$\frac{\nu(As_2S_3)^a}{\nu(As_2O_3)}$
Raman	ir	Raman	
174	140	136	0.79
192	159	154	0.82
217	179	181	0.83
260	198	204	0.77
285	...	244	0.86
331	278	...	0.84
	279	...	0.84
357	299	213	0.83
	311	311	0.87
426	...	345	0.81
	354	355	0.83
461	375	...	0.81
	383	382	0.83

^aThe mean scaling factor is 0.82.

Davydov doublet for which the ir member is found in the infrared reflectivity measurements reported by Zallen *et al.*,⁶ and measured with radiation polarized parallel to the As_2S_3 layer plane.

Branching arrows are indicated at 331, 357, 426, and 461 cm^{-1} where the oxide frequency scales closely to either of two sulfide frequencies, indicating the presence of unresolved features in the recorded spectrum of As_2O_3 . According to the selection rules of Fig. 2, the ir components tabulated in Table II exhibit B_u symmetry and can be assigned Raman-active Davydov partners belonging to species A_g . These, in turn, correlate with layer vibrations A' . (The As_2O_3 Raman line at 288 cm^{-1} was labeled A_g according to our polarization results.) Thus 13 frequencies A_g of A' layer parentage have been located; this is precisely the number expected.

Arsenolite or cubic As_2O_3 (space group $O_h^4-Fd\bar{3}m$) has been previously studied both crystallographically and optically.^{14,15} The cubic unit cell of lattice constant $a_0 = 11.07$ Å consists of eight As_4O_6 molecules, each centered at a site that would be occupied by a carbon atom in a diamond lattice scaled to the new cell dimensions. The As_4O_6 entity is identical to an arsenic trioxide vapor molecule, possessing point symmetry T_d . The oxygen atoms occupy the vertices of an octagon inside of which is a tetrahedron of arsenic atoms. The intramolecular distances O-O = 2.73 Å, As-As = 3.23 Å, and As-O = 1.80 Å unambiguously define the As_4O_6 units which approach each other at a minimum O-O separation of 2.83 Å. The As_2O_3 pyramidal angle O-As-O (98.6°), the As-O-As bond angle (128.2°), and the As-O bond length (1.80 Å) are remarkably preserved in nearly every phase of As_2O_3 , and account for some of the closely comparable features of the

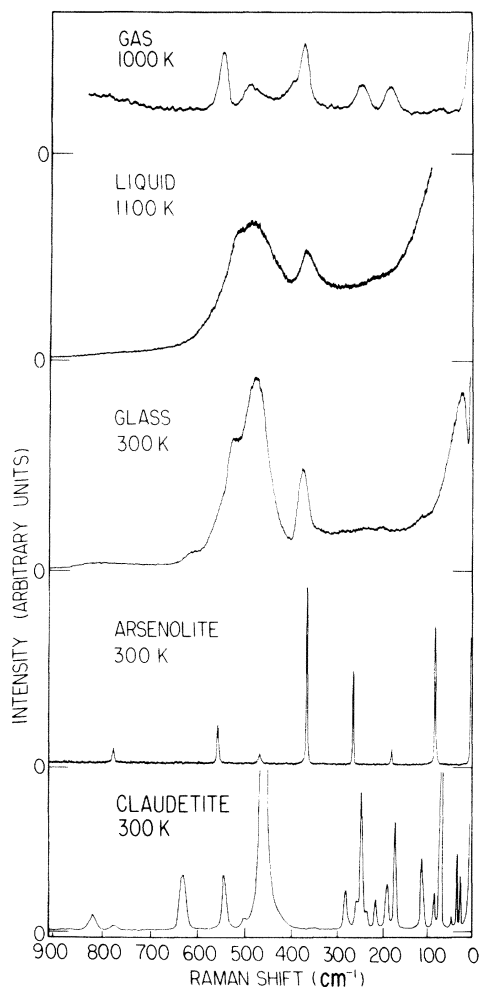


FIG. 5. Raman spectra of all five phases of As_2O_3 .

various vibrational spectra.

The Raman spectra of arsenolite and the other four phases of arsenic trioxide, studied in this paper and the preceding paper, are displayed for comparison in Fig. 5. The arsenolite spectrum reported here is in complete agreement with the published results of Beattie and co-workers.¹⁵ The gaseous, liquid, cubic, and monoclinic phases all exhibit modes which agree in position rather closely with vibrations of vitreous As_2O_3 .¹⁶ Each mode is labeled by its frequency (given in cm^{-1}), symmetry species, and polarization (polarized-p or depolarized-dp), and listed accordingly in Table III. The modes of arsenolite and As_4O_6 vapor included in Table III are alike in frequency, symmetry, and polarization.¹⁵

The significance of recurring bands rests in their correlation with structural units which persist throughout several phases of the As_2O_3 system. One can infer nothing about an observed normal vibration in a particular phase by merely citing its

proximity in frequency to a band in a different phase the structural origin of which is understood, although some authors have concluded otherwise. Bertoluzza,¹⁷ for one, argued that recurring frequencies in the Raman spectra of cubic, monoclinic, and vitreous As_2O_3 were definitive evidence of structural similarities. The A_1 "water molecule" mode of the glass at 50-cm^{-1} and the 49-cm^{-1} B_g rigid-layer mode of claudetite are structurally unrelated and provide a counterexample. Moreover, the 470- and 560-cm^{-1} features in the arsenolite spectrum cannot be identified with the 496- and 555-cm^{-1} bands of the glass inasmuch as the modes of the glass and these particular modes of arsenolite possess conflicting polarization properties. The behavior of autonomous structural units must be manifested in both the symmetry and frequency of those normal modes of the macroscopic system to which they give rise.

According to the above criteria, the spectrum of claudetite exhibits vibrational features which match those of the glass in frequency and depolarization characteristics for seven of the nine bands listed in Table III.

IV. CONCLUSIONS

The vibrational spectrum of claudetite is dominated by its layered structure, as evidenced by

TABLE III. Recurring bands in the five phases of As_2O_3 . Frequencies are listed below in cm^{-1} . Polarization characteristics are indicated in parentheses to the right of the symmetry species.

Glass ^a	Vapor ^b	Arsenolite	Claudetite	Liquid ^c
$50 A_1$ (p) As-O-As	$55 B_g$ (dp)	...
$125 A_1$ (p) AsO ₃	$118 B_g$ (dp)	125 (p)
$250 E$ (dp) AsO ₃	$253 F_2$ (dp)	$269 F_2$ (dp)	$252 B_g$ (dp)	220 (dp)
$370 A_1$ (p) As-O-As	$381 A_1$ (p)	$371 A_1$ (p)	$360 A_g$ (p)	370 (p)
$480 A_1$ (p) AsO ₃	$496 F_2$ (dp)	$470 F_2$ (dp)	$464 A_g$ (p)	480 (p)
$525 E$ (dp) AsO ₃	$504 B_g$ (dp)	525 (dp)
$570 A''$ (dp)	$556 A_1$ (p)	$560 A_1$ (p)	$548 B_g$ (dp)	520 (p)
Intermolecular coupling				
$625 B_2$ (dp) As-O-As	$636 B_g$ (dp)	625 (p)
800 (dp) As ₄ Linkage	...	$782 F_2$ (dp)	$777 B_g$ (dp)	800 (dp)

^aEach band in the glass is associated with one of several structural units described in Ref. 16 and labeled here accordingly.

^bReference 15 and preceding paper.

^cFrom preceding paper. See, in particular, Figs. 8 and 12.

the closely spaced Raman-ir doublets and low-lying rigid-layer modes. It is precisely the weakness of the interlayer interaction that renders the rigid-layer modes distinguishable from the more tightly bound in-plane modes. Thus, a direct comparison of interlayer and intralayer frequencies reveals that the layer-layer binding is weaker than that of the layer network by two orders of magnitude. A detailed discussion of this topic is found in Ref. 8.

Intercrystal frequency scaling between claudetite and monoclinic crystals of As_2S_3 and As_2Se_3 can only be interpreted qualitatively in terms of structural units that retain their identity in the complex molecular layers they compose. The

AsO_3 pyramidal unit and the As_2O water molecule are well-defined constituents of all five phases of arsenic trioxide with which the modes of vitreous As_2O_3 have been explicitly correlated. Close correspondence between the modes of the glass and several modes of claudetite is a manifestation of residual layered structure in the glass, and reflects the existence of identifiable subunits which compose the claudetite layer.

ACKNOWLEDGMENTS

We thank Gerald Reedy at ANL for his help in recording the infrared data. One of us (E. J. F.) thanks Dr. Joseph Pluth for instruction in use of the Buerger precession camera.

*Research supported by the U. S. AEC General support of the Materials Research Laboratory of the University of Chicago by the NSF is also acknowledged.

¹M. J. Buerger, *X-Ray Crystallography* (Wiley, New York, 1942).

²J. F. Nye, *Physical Properties of Crystals* (Clarendon, Oxford, 1957).

³D. M. Hwang and S. A. Solin, *Phys. Rev. B* **7**, 843 (1973).

⁴Natural crystals of claudetite were supplied by Mr. J. S. White of the Smithsonian Institute. The sample sent to us was catalogued R1736 by the Smithsonian Institute.

⁵E. A. Wood, *Bell. Syst. Tech. J.* **43**, 541 (1964).

⁶R. Zallen, M. L. Slade, and A. T. Ward, *Phys. Rev. B* **3**, 4257 (1971).

⁷E. B. Wilson, J. C. Decius, and P. C. Cross, *Molecular Vibrations* (McGraw-Hill, New York, 1955), p. 335.

⁸R. Zallen and M. L. Slade, *Phys. Rev. B* **9**, 1627 (1974).

⁹R. C. Weast, *Handbook of Chemistry and Physics* (The Chemical Rubber Co., Cleveland, 1971), p. B-69.

¹⁰D. M. Hwang and S. A. Solin, *Appl. Phys. Lett.* **20**, 181 (1972).

¹¹G. Herzberg, *Molecular Vibrations* (Van Nostrand, Princeton, 1945), Vol. 2, pp. 175-177.

¹²A. A. Vaipolin, *Kristallografiya* **10**, 596 (1965) [*Sov. Phys.-Crystallogr.* **10**, 509 (1966)]. The AsX_3 units are slightly distorted in arsenic selenide. Each of the two inequivalent arsenic atoms exhibits three unequal Se-S-Se valence angles which yield an average of 98° . A similar situation obtains in As_2S_3 and As_2O_3 (see Ref. 13).

¹³A. F. Wells, *Structural Inorganic Chemistry* (Oxford U.P., Oxford, 1962), pp. 668 and 683.

¹⁴Ralph W. G. Wyckoff, *Crystal Structures* (Interscience, New York, 1964), pp. 17-19.

¹⁵I. R. Beattie, K. M. S. Livingston, G. A. Ozin, and D. J. Reynolds, *J. Chem. Soc.* **1970**, 449.

¹⁶G. N. Papatheodorou and S. A. Solin, *Solid State Commun.* **16**, 5 (1975).

¹⁷A. Bertoluzza, M. A. Morrelli, and C. Fagnano, *Lincei Rend. Sci. Fis. Mat. Nat. (Italy)* **52**, 923 (1972).

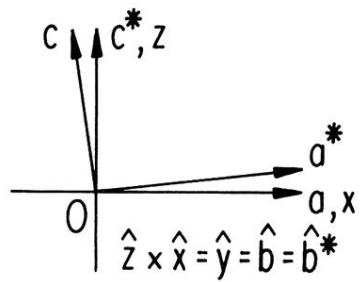


FIG. 1. Orientation photograph of claudetite. Below the x-ray photograph, the crystallographic axes are referred to a set of Cartesian coordinates (xyz) . Asterisks label directions in reciprocal space. Angle $c0a = 94^\circ$.